IMPACT DAMAGE BEHAVIOR AND NON-DESTRUCTIVE INSPECTION METHODS OF THIN HYBRID CARBON-FLAX LAMINATES

K. Strohrmann[1], J. Blaut[1], C. Panescu[2], H.-J. Endres[2], R. Svidler[3], M. Hajek[1]
[1]Technische Universität München, Arcisstraße 21, 80333 München, Germany;
[2]Hochschule Hannover, Heisterbergallee 12, 30453 Hannover, Germany;
[3]Technische Universität Chemnitz, Straße der Nationen 62, 09111 Chemnitz, Germany

Abstract

This work investigates the use of flax fibers in aerospace applications, focusing on the properties of impact energy absorption and non-destructive testing (NDT) methods in terms of greener aerospace and good energy absorption properties. The specimens investigated were double layered woven fabrics made of carbon (C) and flax (F). The materials were carbon, plain weave, 200 g/m² and flax, twill weave, 100 g/m², 150 g/m² and 200 g/m². Laminates were fabricated with a vacuum infusion technique using an epoxy bio resins glue (Super Sap), which is 19% bio-based. The quality of the fiber-matrix bonding within the different laminates was analyzed with the imaging technique computer tomography. The analysis of impact damage was performed on energy dissipation, optical appearance, depth and size. In order to identify the damaged area within the material and find out about the applicability, the NDT methods “Ultrasonic Echo Analysis” and “Vibration-Induced Thermographic Inspection” were attempted. The results showed that of the three flax weaves, the 150 g/m² flax weave performed the best mechanically in hybrid and pure laminates. Furthermore, the stacking sequence of the hybrid laminates showed an effect on the damage behavior, as [C/F] laminates showed small damage up to 1.5 J, while [F/C] specimens were damaged completely. The Ultrasonic Echo Analysis was applied to pure flax and hybrid specimens, with acceptable interpretability. Vibration-induced thermography was barely interpretable, but showed better results when filming the carbon side of the hybrid specimens.

1. INTRODUCTION

With funding from BMWi LUFO V-2, the project „InteReSt“ investigates the potential of hybrid natural and carbon fiber reinforced plastics (NFRP and CFRP) as structural composite materials used in aerospace applications, especially in semi-structural parts of helicopters.
In previous studies the flax fiber turned out to be the most promising natural fiber for our investigations, due to its high specific strength and stiffness compared to other natural fibers [1]. Another positive aspect is the smaller ecological footprint which originates mainly from the lower energy input compared to carbon fiber during the production process [2]. Furthermore, the lightweight potential is high, as flax fibers have a lower density than conventional fibers (such as glass and carbon), and their mechanical properties are comparable to glass [3]. Additionally, the energy dissipation properties of flax fibers have been emphasized in different sources, where very good vibrational damping, crash absorbing and impact resistance properties were observed. [4], [5], [6], [7], [8].
Only little research has been conducted on the hybrid use of flax and carbon fibers in an epoxy resin matrix. References cover to some extent the impact and damping behavior of multi-layered hybrid materials. Investigations of very thin laminates with only two layers and a total thickness between 0.45 and 1.75 mm, as in our investigations, are rarely performed.
Hybrid flax laminates are promising for secondary structural parts that require good temperature and acoustic insulation properties, therefore the area of application is envisioned in panel and casing structures. These parts are often prone to impact loads from the outer environment of the air vehicle. Flax fibers may offer good impact damage behavior in terms of energy dissipation due to internal friction.
In ultralight applications the mass is an important design parameter, so the mass-beneficial or neutral substitution of carbon layers by flax layers is aimed in this project. Associated adverse effects in strength and stiffness need further multidisciplinary consideration
Furthermore, the NDT methods “Ultrasonic Echo Analysis” and “Vibration-Induced Thermographic Inspection” were applied to the damaged specimens. These NDT methods are commonly used in the aerospace sector, especially for the detection of barely visible impact damages in maintenance and for assessing quality assurance.

1.1. Energy Dissipation in Flax Fibers

Flax is a plant, from which technical fibers with an average diameter of 19 µm and a length of 25-120 cm can be extracted by a drying and mechanical treatment process [9]. FIG 1 a) shows the flax plant after harvesting a tuft off the field, and b) a twill weave made from flax fibers.

a) b)

FIG 1: Flax a) Flax plant, harvested [10] b) Flax woven fabric [11].

As the fibers are neither synthetically produced nor endless, the production process mostly requires a yarn. In this process, several fibers are twisted, so a twill fabric as shown in FIG 1 b) can be produced. The fabrics available currently are limited in smaller scales to an areal density of about 100 g/m².
The use of flax is supported by the political and ecological interest of greener aerospace. The weight-saving potential and the better carbon footprint as well as energy efficiency compared to carbon are supportive arguments [12].
TAB 1 provides an overview of selected ecologic and economic properties of carbon, flax and glass composites. The data were mostly acquired with the software GABI and compared and combined with other sources [13].

	Unit	Carbon	Glass	Flax
Carbon footprint fiber	(CO_2)kg/ (fiber)kg	19.98	2.79	-1.37
Energy consumption fiber	MJ/kg	361.92	35	3.92
Energy consumption laminate	MJ/kg	345	85.3	52.3
Costs	€/5 m²	104.60	13.10	92.60

TAB 1: Ecologic and economic properties of carbon, glass and flax-reinforced plastics [14], [15]

As the values show, there is the high potential for ecological benefits by replacing low lifecycle performance fibers with flax. Because of the lower mechanical properties, the substitution is only taken into account for secondary structural applications.

1.2. Literature Review of Impact Damage in Flax Fibers and Hybrids

In the literature, impact studies have been conducted on pure flax and hybrid carbon-flax composites, focusing mainly on laminates with a thickness > 2 mm. Selected results are described in the following text.
Y. Lebaupin et al. [6] worked on the impact behavior of different flax layups and fiber orientations. They used eight layers of unidirectional (UD) flax with an areal density of 450 g/m², the lay-ups were: $[0]_8$, $[0/90]_4$, $[0_2/90_2]_S$, $[-45/0/45/90]_S$. The laminates were subjected to a low velocity impact of 3.6 J followed by tensile and compression tests. The results showed that the quasi-isotropic laminate was least sensitive to the impact load; and most of the laminates did not show significant loss of mechanical properties.
F. Sarasini et al. [16] aimed for a hybrid laminate which should be environmentally sustainable, cost effective and better able to sustain impact damage than CFRP. They investigated a UD flax-carbon laminate with 14–18 layers and layup orders of $[F]_3$, $[C]_3$, [C/F/C] and [F/C/F]. A four-point bending test was performed, as well as an impact damage test with energies between 5-30 J. The damaged probes were tested in tensile and bending tests. With the use of micro-thermography it was shown that the pure CFRP laminates were more sensitive to impact damage than the hybrid ones. Furthermore, the [F/C/F] layup showed better resistance to the impact than the [C/F/C], and the [C/F/C] laminates showed a better behavior in terms of bending stiffness.
V. Fiore et al. [17] investigated in their work the mechanical properties of two different flax weave fabrics with a reinforcing UD layer of carbon. The flax weave types were 220 g/m² twill weave and 150 g/m² plain weave. These specimens were made of six layers, either $[F]_6$ or $[C/F_2]_S$. A three-point bending test and a tensile test were performed. The results showed that in terms of bending stiffness the plain weave performed better, while in terms of tensile properties the twill weave superceded. It was pointed out, that the pure flax specimens were not sufficient for structural demands, but the carbon reinforcement strengthened the laminates significantly. Thus, the plain weave of 150 g/m² showed better results and made a structurally useful laminate.
Petrucci et al. [18] performed impact testing on hybrid laminates including glass, hemp, basalt and flax. The fact that the performance of the hybrid laminates including flax was in most cases superior to laminates without flax, indicates the potential of flax-based hybrids for impact loads.

2. IMPACT DAMAGE TESTING

The following sections describe the tests and analysis performed within this work. Firstly the materials, consisting of fibers, matrix and its processing parameters, are characterized. Therefore, generic sheets of six plies were made and tested on basic mechanical properties.
The resulting laminate properties of the impact specimen and the experimental setup are described afterwards

2.1. Materials

FRP are two-component materials made of a matrix and a fiber, which are typically either unidirectional aligned, woven to fabrics, laid in webs or as processed braidings. In this work, woven fabrics were used, suitable for complex shell structures and thin-walled parts.
Woven fabrics consist of at least two yarn systems, warp and weft, which are orthogonally crossing each other. The weave binding is described by the crossing order of the weave and influences the properties of the laminate. Atlas, twill and plain weave are the standard weave bindings in FRP [19].
In this case, plain and twill weave fabrics were used. Characteristically for plain weaves, the weft yarns are crossing each warp yarn. In comparison, twill weave is where the weft yarn skips two to three yarns before crossing the warp yarn, which keeps the yarns straighter and thus, the laminate has higher mechanical strength and stiffness [19].
The used materials were carbon, plain weave, 200 g/m² and flax, twill weave, 100 g/m², 150 g/m² and 200 g/m². The materials fabricated by Lineo were surface-treated and the Composite Evolution fibers were not. Further details are listed in TAB 2.

Material	Specification	Weave Binding	Manufacturer
Flax	FlaxPLY BL 150	Twill	Lineo
Flax	FlaxPLY BL 200	Twill	Lineo
Flax	Biotex Flax 100 g/m² 2x2	Twill	Composite Evolution
Carbon	HP-P200C	Plain	HP Textiles

TAB 2: Fabric material details [11], [20], [4], [21]

The woven fabrics were consolidated to a laminate with a partly bio-based epoxy resin glue, described in TAB 3. Epoxy resin is a thermoset matrix, which is chemically closely cross-linked and form-stable at a broad range of temperatures [22].
The Super Sap Epoxy contains 19% bio-based components which drop off either as co-products or as waste of other industrial processes, such as the bio-fuel production. Additionally Super Sap has no color, is UV-resistant and has low viscosity, which makes it suitable for vacuum infusion processing [23].

Matrix	Manu-facturer.	Mixing ratio	Curing cycle
Super Sap ® CLR INF Hardener	Entropy Resins	100:33	24h @ RT or 2h @ 120°C

TAB 3: Matrix material details [23]

2.1.1. Vacuum Injection Molding

The thermoset FRP were produced with vacuum injection molding. Thereby, VARI (vacuum assisted resin infusion) was used, which works with dry fabrics applied on a release waxed surface. A flow aid and the resin feed as well as the vacuum connection were sealed with a seal tape and foil.
Resin was injected using vacuum and gravity. The injection speed is an important variable for the results of fiber matrix bonding and the amount of voids, as well as the vacuum tightness.
The curing as cross-linking reaction was initiated by temperature while the vacuum was still maintained. The curing time is defined by the resin curing cycle, see TAB 3. Due to the high cycle times, this method is only suitable for low batch sizes and rather large structures [24].
The advantage of injection molding is that the weave and the matrix are design variables, the combinations of diverse bio-based epoxy resins and weaves can be tailored compared to prepregs, where the material combination is set.
The production of the vacuum-infused laminates and the pretesting of the laminate properties in the following section was conducted by the Institute of Bioplastics and Biocomposites at Hochschule Hannover.

2.1.2. Laminate Properties

The homogeneous materials flax unidirectional, flax woven and carbon woven were preliminarily tested in six-layered laminate probes. The results in TAB 4 for flax 150 g/m², 200 g/m² and carbon 200 g/m² were averaged on the basis of ten specimens, the results for 100 g/m² were based on five specimens.

The results indicate, that the density of each flax weave laminate is lower than the carbon laminate. Also, as expected, the carbon is showing better specific properties. In terms of quality, the processing of flax needs to improve in order to increase the fiber volume content.
It is significant that the 150 g/m² weave is performing better in tensile strength and modulus than the thinner 100 g/m² weave and the thicker 200 g/m² weave. A similar trend was discovered in the impact load tests.
As shown later by FIG 2 “Computer Tomographic Inspection”, the weave size of the 200 g/m² weave is large, which leads to a low volumetric density.
The tensile modulus of 100 g/m² and 150 g/m² flax weave was nearly the same, which is explained by the low twist in these lighter weaves, compared to the 200 g/m².

	Unit	Flax 100	Flax 150	Flax 200	Carbon 200
Density[1]	g/cm³	1.257[2]	1.257	1.235	1.492
Tensile strength[1]	MPa	75.8	103.2	75.8	536.7
Tensile modulus[1]	GPa	8.390	8.702	4.639	37.690
Specific strength[2]	MPa/ g/cm³	60.33	82.10	61.38	359.72
Specific modulus[2]	GPa/ g/cm³	6.677	6.923	3.757	25.261
Maximum strain[1]	%	-	1.85	2.66	1.60
Fiber volume fraction[2]	%	26.71	36.34	25.34	49.13
Bio-based mass[2]	%	44.92	53.43	42.90	7.41

TAB 4: Mechanical properties of pure flax and carbon laminates
[1] experimental results
[2] calculated values

The ratio of bio-based mass as $\frac{m_{bio}}{m}$ is calculated as shown in equation (1):

$$\frac{m_{bio}}{m} = \frac{m_F}{m} * BR_F + \frac{m_M}{m} * BR_M \quad (1)$$

With F indicating fiber, M indicating matrix and BR as bio-based ratio. BR_F is thereby either 100% (F) or 0% (C) and the BR_M is for all laminates 19 % regarding the Super Sap epoxy matrix. Therefore, the carbon laminate is also listed as partly bio-based.

2.1.3. Computer Tomographic Scans

The computer tomographic scans show clearly the weave pattern by different gray scales for fibers and matrix. When comparing the different materials in FIG 2, carbon 200 g/m², flax 200 g/m² and flax 150 g/m², the different fiber-volume

contents were observed again. It can be seen that the mesh and yarn size of the 200 g/m² flax weave are big and show large interspaces explaining the low fiber volume fraction. Additionally, air inclusions within the twisted yarn can be seen in the out-of-plane view of flax 200 g/m².

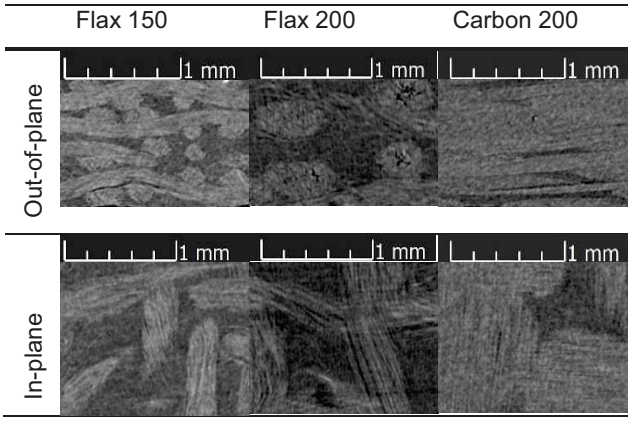

FIG 2: Computer tomographic scan of carbon laminate 200 g/m², flax 150 g/m² and flax 200 g/m², in cross sections

In comparison to the other flax laminates, the 150 g/m² scan shows a neater weave, which leads to the better mechanical values.
The carbon weave barely shows any interspaces and the fiber bundles are neatly compacted, which explains the highest fiber volume content in this material.

2.2. Specimens

The produced and tested laminates are listed in the following table, TAB 5. Each of the listed laminates was used for four specimen, 145 mm x 100 mm in size, but for the pretest material $[F]_3$, only three specimens were tested. The materials used, fibers and matrix, respectively, are described in the following sections.

Specification	Layers	Stack-up (top-bottom)	Areal density (flax) [g/m²]	Batch	Density [kg/m³]	Fiber volume fraction [%]
FF_200_A	2	$[F]_2$	200	A	1.20	24
FC_200_A	2	[F/C]	200	A	1.26	30
CF_200_A	2	[C/F]	200	A	1.27	30
CC_200_A	2	$[C]_2$	200	A	1.45	49
FF_150_B	2	$[F]_2$	150	B	1.24	35
FC_150_B	2	[F/C]	150	B	1.22	38
FF_100_B	2	$[F]_2$	100	B	1.26	26
FF_200_B	2	$[F]_2$	200	B	1.19	23
CC_200_B	2	$[C]_2$	200	B	1.48	48
FFF_200_B	3	$[F]_3$	200	B	1.19	29

TAB 5: Overview of laminates and their defining properties and densities

The fiber volume content φ of the specimens was calculated with the assumption of a flax fiber density of 1.44 g/cm³, carbon fiber density of 1.8 g/cm² and matrix density of 1.1 g/m² using the following equation (2):

$$\varphi = \frac{\sum_{i=1}^{n} \frac{m_i}{\rho_i}}{\sum_{i=1}^{n} \left(\frac{m_i}{\rho_i}\right) + \frac{m - \sum_{i=1}^{n} m_i}{\rho_M}} \quad (2)$$

i is indicating the layer and M is indicating the matrix. The fiber masses of each layer m_i were calculated with the areal density.
FIG 3 shows the surface of four exemplary stack-ups of the specimen.

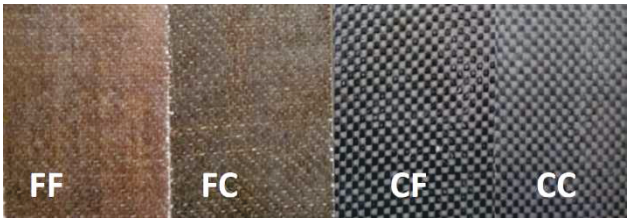

FIG 3: Appearance of different laminate stack-ups with 200 g/m² flax and carbon weave

2.3. Experimental Setup

The impact damage application and the NDT analyses were performed at the testing facility of the Chair of Lightweight Structures at the Technical University of Munich. The specimens were preconditioned for 24 h at 23°C and 50% relative humidity, as polymers and flax fibers are sensitive to environmental conditions.
The impact tower was set according to DIN EN 6038. The tests were conducted using a hemispherical steel impactor with a diameter of 16 mm and a mass of 2.4993 kg. During impact testing, an acceleration sensor records the acceleration of the impactor over time. Two light barriers were used to determine the velocity right before and after the impact. Based on these two velocities and the mass of the impactor, the dissipated energy was calculated.
The clamping device is made of a steel base plate with four clamps on it. In the middle of the base plate there is a 67 mm x 127 mm cutout. The specimens were centered on the clamping device using pins.
After a pretest with an energy level of 1 J and the clamping device set according to DIN EN 6038, the very thin specimens tended to bulge out of the clamping device. In order to avoid this behavior, a lengthwise strengthened fixation by frame rails was used in all further tests.
With respect to the several layups, different impact energy levels were used. The pure carbon laminates were impacted at 1 J, 2 J and 3 J, the pure flax laminates showed a bigger damage in the pre-test, so the following impact energy levels where chosen at 0.5 J, 1 J and 2 J. For the hybrid specimens of the first batch with an areal density of 200 g/m², the used impact energy levels were 1 J, 1.5 J and 2 J. The hybrid laminates of the second batch with an areal density of 150 g/m² were impacted at 1 J, 2 J and 3 J. TAB 6 shows an overview of the different impact energy levels and the damage appearance of all specimens. In order to clarify the different fixation methods at the pretest, “(pre)” was added to the specification of these results, which showed less damage than the results with the improved fixation.

In all tests, the aimed impact energy was verified by assessing the kinetic energy through the light barrier signal shortly before impact. In all tests, a maximum deviation of ±0.15 J was achieved.

3. RESULTS

After the low velocity impact, the induced damage was inspected and characterized. The results in terms of signal analysis, optical appearance, depths and NDT analysis are described in the following sections.

3.1. Visible Damage Characterization

The visual inspection characterized the failure mode of the specimens listed in TAB 6. The carbon specimens showed first failures at an impact energy level of 2 J. The damage to the carbon material was small and barely visible. For the flax specimens, damage occurred at all impact energy levels. Generally, for symmetrically woven fabrics, a cross-shaped failure was characteristic. The specimens with lower areal density were largely disrupted by the impactor and showed anti-symmetric failure modes.
For the hybrid specimens with an areal density of 200 g/m², the stacking sequence had an effect on the failure mode and the severity of the damage. For an [F/C] stacking sequence, no failure occurred at 1 J impact energy within the pretest. Using the optimized fixation, a round failure occurred at energy levels of 1 J, 1.5 J and 2 J.
The mirrored stacking sequence ([C/F]) showed a small dot-shaped failure at an energy level of 1 J. No severe damage was observed up to 1.5 J. At an impact energy of 2 J, a total failure of asymmetric shape occurred.

+	cross-shaped	*	asymmetric failure
—	horizontal failure	|	transversal failure
•	dot-shaped failure	○	round failure
nF	no failure		(empty) not specified

Speci-fication	1 J (pre)	0.5 J	1 J	1.5 J	2 J	3 J
FFF_200_B	+ /+				+	
FF_100_B	|	*	*		*	
FF_150_B	+	+	+		*	
FF_200_B	+	+	+		+	
FF_200_A	*	+	+		+	
FC_200_A	nF		○	○	○	
CF_200_A	•		•	•	*	
FC_150_B	nF		nF		nF	*
CC_200_A	nF		nF		•	*
CC_200_B	nF		nF		•	—

TAB 6: Overview of damage characterization

The $[F]_3$ layered material was used for the setup and pretests, and two specimen were tested at 1 J, both showing a cross-shaped failure.
Exemplary pictures of the listed failure characterizations are shown in FIG 4.

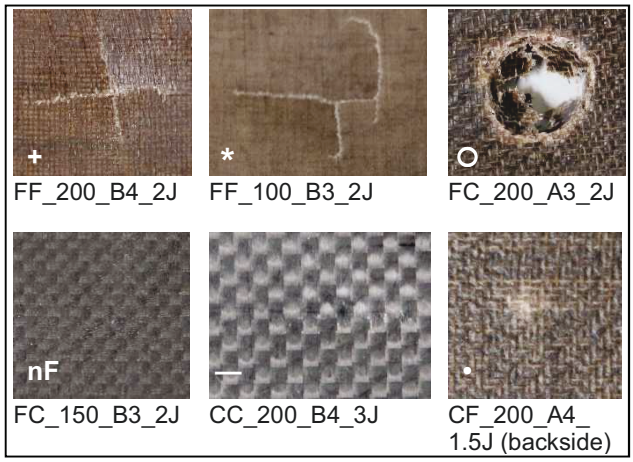

FIG 4: Different damage characterization

The different failure modes according to the characterization could not be clearly separated for all cases.
The results of the FC_150 laminate are significant, as it was tougher than the CC_200 in the case of 2 J impact energy. There was no visible failure, and failure was also not detected with the NDT methods. This might be due to the more elastic behavior of the laminate. In addition, the friction of the fixation might have absorbed additional energy in this case due to the small thickness. For a better understanding, more tests need to be conducted.
Another significant result was the very different behavior of the [C/F] and [F/C] stacking with 200 g/m² weave of flax and carbon. As shown in FIG 4 and TAB 6, the [C/F] layup showed less fracture damage than the [F/C] layup and up to 1.5 J only a small area was damaged. This is explained by the bending stress during the impact, which applies more load to the lower layer than to the top layer. Increasing energy levels caused large ruptures in both layers.
The damage behavior of the [F/C] laminate can be seen in FIG 5. It is clearly more damaged than the [C/F] laminate, pictured bottom right in FIG 4.

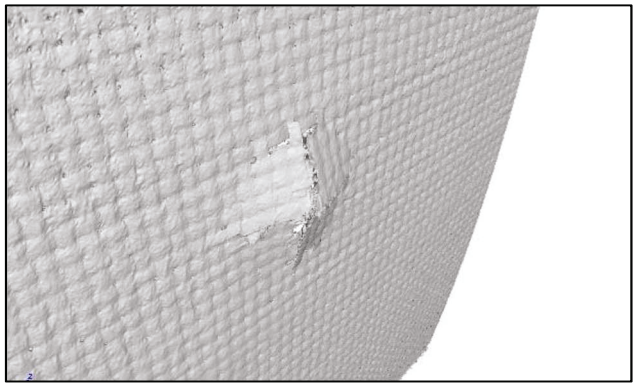

FIG 5: Computer Tomography of FC_200_A4 impacted with 1.5 J

3.2. Depth and Relaxation

With a dial gauge (accuracy of 0.01 mm) the penetration depth directly after the impact is measured ("avg. depth [mm]" in FIG 6). In order to identify the relaxation of the damaged material within a week, the damage depth is measured a second time seven days later.
The difference is averaged in FIG 6 as "avg. relaxation [mm]"; the percentage of the relaxation to the initial depth is also graphed as "avg. relaxation [%]" The values are averaged per laminate type. The modes of "no failure", disrupted failure and relaxation values higher than 100% were excluded.
The damage depth after impact is higher with increasing impact energy level for the same material. In general the relaxation after one week shows a decrease in penetration depth, 12% on average.

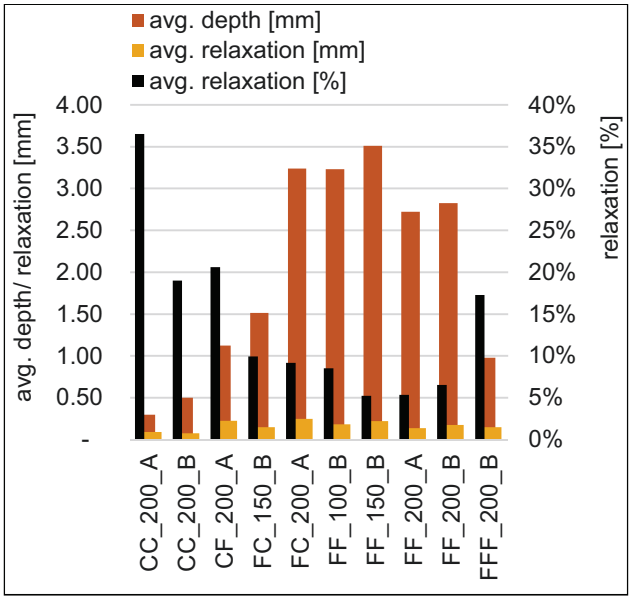

FIG 6: Absolute damage depth and relaxation of depth in [mm] and [%] averaged on type of laminate

It can be seen, that all FRP are showing relaxation processes. In general the damage depth increased with the amount of flax in the laminate, but considering the different energy levels and excluded values, the averaged values are not comparable.
The percentage decrease showed the highest relaxation ratios for carbon specimens, but lowest absolute depth difference. Regarding the lower absolute damage depth and the measurement errors, the relaxation is attributed as a mainly matrix driven phenomenon and shows no dependence on the fiber material.

3.3. Dissipated Energy

During the low velocity impact, the acceleration of the impactor was recorded. Using the impactor mass and the measured acceleration, the impact force on the specimens could be determined. FIG 7 shows an exemplary acceleration curve on a hybrid [C/F] layered 200 g/m² specimen.
The signal of the acceleration sensor shows a static noise in the range of ± 0.2 g, the offset at the initial time is showing the 1 g gravity acceleration.
The characteristic behavior of the acceleration shows an increase to a maximum value and then a decrease back to zero in an anti-symmetric curve, where the ascent is typically steeper than the descent, depending on the absorbed energy. The scatter on the acceleration curve provides a clue about the extent of the damage, as well as the absorbed energy.
Appearing peaks indicate failure, such as fiber-bundle breakage or delamination. Typically, these scattering peaks appear around maximum acceleration. Specimens with no damage showed a smooth acceleration curve with no prominent peaks. The acceleration curves were used to validate the optical definition of failure/no failure. Maximum acceleration of all specimen was also considered, but no conclusions were drawn from this analysis.

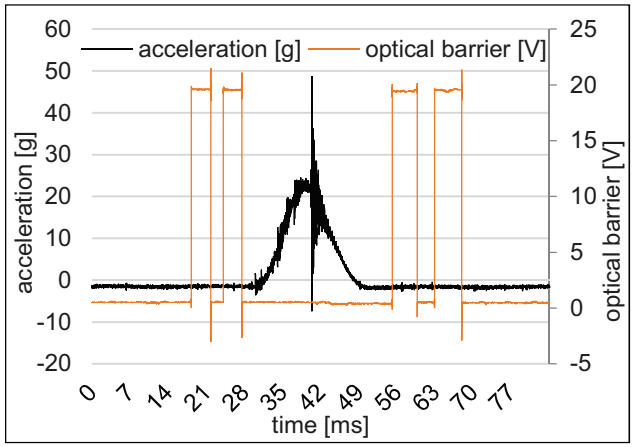

FIG 7: Acceleration curve during impact on CF_200_A_4 with 1.5 J

3.4. Non-Destructive Testing Methods

NDT is used in FRP quality assurance and maintenance of structural parts in the aerospace sector. In order to enhance the knowledge and applicability of natural fibers, these methods were applied on damaged specimen with either visible, barely visible or non-visible damage.

3.4.1. Ultrasonic Echo Analysis

The ultrasonic echo analysis was performed by a 3-axis scanner with a 3 MHz test probe and the software HILLGUS for results analysis. The investigated area was 70 mm x 100 mm in size, and a grid with 0.25 mm increments in the X and Y directions was used. At the beginning, a volume scan of the specimen was performed, which was later used to derive C and D scans of the specimens [25].
The C scan showed the strength of the echo of the input signal, which was reflected at a significant change in speed of sound of the conducting medium. In an undamaged material, this first happened on the specimen's backside, but in the case of delamination or fracture, the signal was reflected earlier. The strength of the echo signal in dB is shown grey scaled in the pixel pattern (see FIG 8). The higher the echo, the less was transmitted through the laminate, , it already gives a clue on the depth of the damage but is not a 3D-view as the D-scan is.

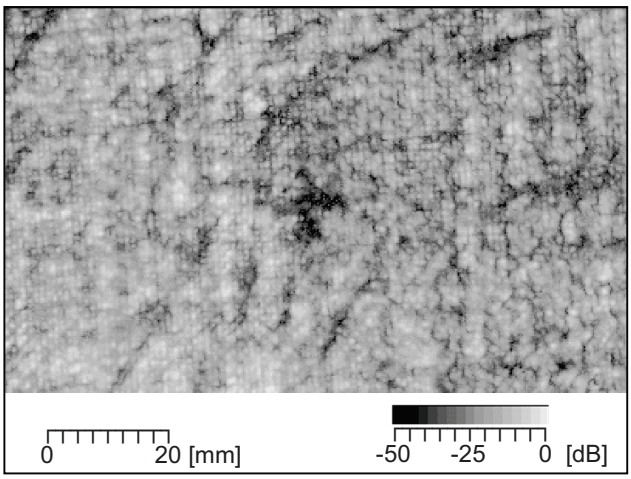

FIG 8: Flax Ultrasonic Inspection, C-Scan of FFF_200_B_1 impacted with an energy level of 1 J, cross-shaped damage

Due to the high deformation of most of the pure flax specimens, the ultrasonic echo analysis could not show the damage properly. Within large deformations, the ultrasonic echo was not vertically reflected by the probe so that the echo signal could not be received.
Nevertheless, the applicability of this inspection method in flax reinforced material was proven by the three layered flax specimens, which showed cross-shaped damage, see FIG 8. The irregularities in the undamaged area of the specimens are due to folds in manufacturing and a variation in thickness, so they should be neglected for the damage characterization.
It should be mentioned that flax fibers display a strong hydrophilic behavior, and the distilled water bath, which was used for ultrasonic inspection, might therefore have an impact [26]. No difficulties or significant influences were detected during the inspection.
For the hybrid carbon-flax specimens, reliable detection of the damage was performed. In FIG 9, the damage of specimen CF_200_A impacted with 1.5 J is shown. The damage was optically visible as dot-shaped damage. This means that with a similar structure, where the backside might not be accessible, maintenance would rely on NDT methods such as Ultrasonic Echo Analysis.
The small black dots in the figure are indicating either air inclusions in the laminate, likely in the flax layer, errors in reflection or interlaminar imperfections.

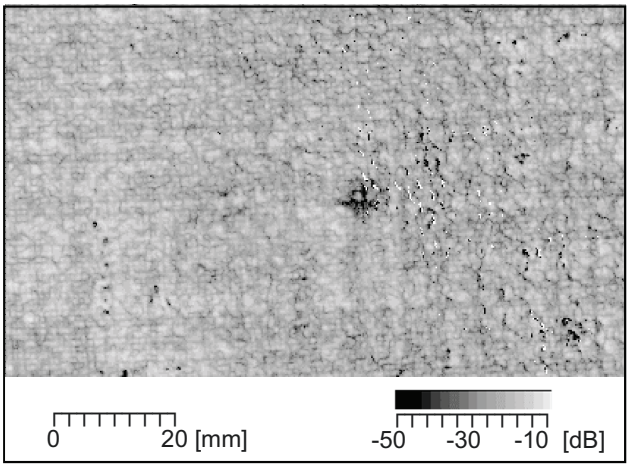

FIG 9: Hybrid Ultrasonic Inspection, C-Scan of CF_200_A_4_1.5J (F)

3.4.2. Vibration-Induced Thermography

For the vibration-induced thermographic inspection, the specimens were stimulated by ultrasonic vibration with 40.8 kHz for 0.6 ms. This vibration was dynamically transmitted through the material and open fractures or debonded layers were heated up due to the resulting friction. This friction heat can be seen in comparison to material at ambient temperature.
An infrared video camera in combination with the software IRControl V4.53 were used for video imaging with a duration of 3 s; afterwards, the most significant pictures were interpreted.
The damage of the pure carbon specimen CC_200_B, impacted at 3 J, is thermographically imaged in FIG 10.
The lower bright point was caused by the stimulation with ultrasonic vibration. In the middle of the figure, the horizontal failure is visible.

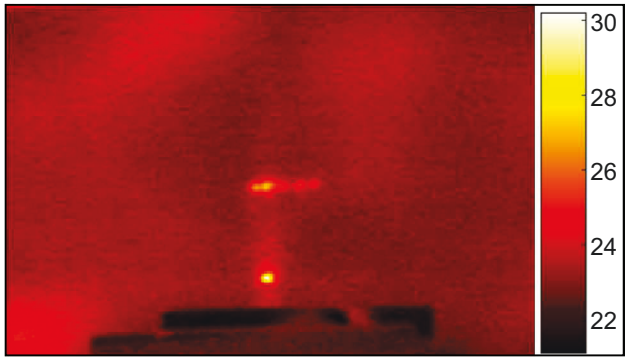

FIG 10: Thermographic image of the CC_200_B4 specimen, impact level 3 J, horizontal fracture, scale in [°C]

FIG 11 shows the infrared picture of specimen FF_200_B, impacted with 0.5 J. The stimulation point is clearly visible and the cross-shaped damage is barely visible, only the horizontal crack can be seen. The reason could be the good damping properties of flax material, which damps due to internal friction in the yarns and fibers. The temperature contrast, caused by the additional friction on the open crack surfaces, is thereby negligible and barely visible.
Compared to FIG 10, showing the pure carbon probe, the mean temperature of the flax probe was about 24°C with peaks of 25°C. Within the carbon, the mean temperature was roughly one degree lower, which supports the hypothesis.
Furthermore, there were standing waves in a circular pattern around the stimulation. This phenomenon also appears in CFRP laminates, if the stimulating frequency is close to an eigenfrequency. In this case the vibrating waves cause a temperature increase in the pattern of the resonance mode.
The blurry larger dots are assumed to be hand-warmed finger prints, due to handling the specimen shortly before testing.

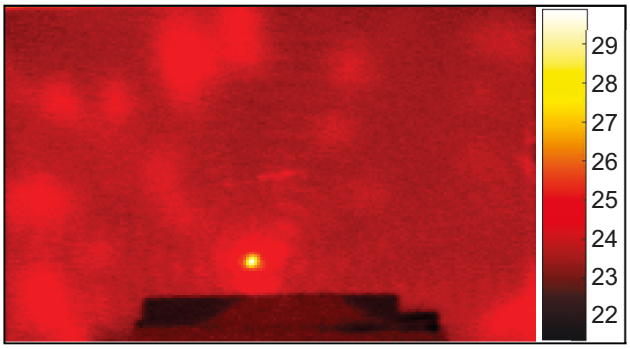

FIG 11: Thermographic image of the FF_200_B4 specimen, impact level 1 J, cross shaped failure, scale in [°C]

Next, FIG 12 shows the infrared picture of the CF_200_A specimen impacted with 1.5 J energy level. The damage in the flax layer is easily visible. But for the same materials in the [F/C] stacking sequence, the results were barely interpretable. This is associated with the layer where the stimulation was coupled into the material. The infrared imaging of damages works slightly better on the C side of the hybrid laminate than on the F side, which is again explained by the higher damping and internal friction in the flax layer.

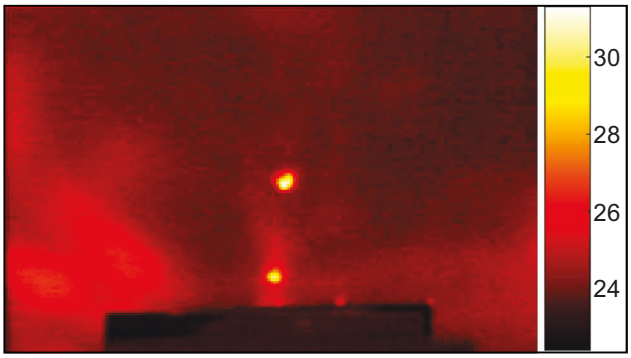

FIG 12: Thermographic image of the CF_200_A4 specimen, impact level 1.5 J, dot shaped failure, scale in [°C]

4. DISCUSSION AND CONCLUSION

The last part is picking up on the noteworthy results and listing them as “key findings”, followed by the conclusions drawn from these findings. Lastly the plans and ideas of future work are presented.

4.1. Key Findings

- Thin laminates with a bio-based mass content of more than 50% were produced
- Hybrid laminates with an impact resistance comparable to pure carbon layers and a bio-based content of over 30% were tested
- In terms of weight reduction, strength, fiber volume content and impact resistance the 150 g/m² weave showed the best properties compared to 200 g/m² carbon weave
- The stack-up order [C/F] (both 200 g/m²) with flax in the lower layer showed smaller damage on impact loads than the [F/C] stack-up (without pretest)
- On 2 J of impact energy load, the FC_150_B laminate showed better damage resistance than the CC_200_B probes
- Ultrasonic Echo Analysis could be applied to thin flax and hybrid carbon-flax laminates with interpretable results
- Vibration-Induced Thermography is barely interpretable for thin flax laminates
- For thermographic imaging of thin hybrid carbon-flax laminates, the interpretability of damage was slightly better when filming the carbon side

4.2. Conclusions

The aim of this paper was to find out about the manufacturability and impact damage behavior of hybrid carbon and flax reinforced plastics, as well as the applicability and interpretability of the NDT methods: Ultrasonic Echo Analysis and Vibration-Induced Thermographic Inspection.
Laminates with different areal density and stack-up orders were produced with vacuum injection molding. These were damaged with an impactor at different energy levels. All laminates investigated were compared in terms of acceleration signal, energy dissipation and damage depth. Certain specimens were chosen to be analyzed with the non-destructive inspection methods.
Firstly hybrid flax-carbon laminates with a thermoset, partly bio-based resin were successfully produced. The highest fiber volume content in flax laminates was achieved with the 150 g/m² weave. The hypothesis is, that less twist of the yarns and the higher fiber volume content compared to the 200 g/m² material lead to better mechanical properties. For the 100 g/m² material the lower strength is explained by the lack of surface treatment.
The best impact resistance and bio-based material was achieved with the hybrid laminates of 150 g/m² flax weave and 200 g/m² carbon. The slightly better performance compared to pure carbon laminate could also be liable to the test setup, where the clamping force was not explicitly adjusted, while insufficient clamping force could lead to energy dissipation by friction within the clamping device.
A different impact resistance behavior with respect to the stacking order of 200 g/m² flax and carbon was observed. While the [F/C] layered laminate was sustaining the impact load in the 1J pretest, the [C/F] layered laminate showed damage. With increasing impact loads, the [F/C] laminate failed completely and the [C/F] layer continued to fail significantly less, up to 1.5 J. With an impact energy of 2 J both stack-ups failed completely.
It could also be shown that non-destructive inspection methods can be applied and interpreted for hybrid carbon flax laminates, when thermographic imaging is used on the carbon side instead of the flax side of the laminate.
Both NDT methods were more complex to evaluate for flax-only laminates, while Ultrasonic Inspection was applicable and interpretable and Thermographic Inspection was evaluated as not recommendable for damage inspection in pure flax laminates.
As a conclusion, for reasons of thickness, mass, strength, stiffness and impact resistance, the 150 g/m² flax weave is the best candidate for substituting 200 g/m² carbon weave layers. As in two layered structures, the scope of tailored design is very limited, and the substitution is only beneficial in a very narrow range of application.

4.3. Future Work

It should be mentioned, that this work was focusing on the feasibility and first glance of impact response. For more reliable results, tests in a statistical scope needs to be performed, especially as the natural fibers offer a higher statistical deviation than conventional fibers.
As impact resistance has an influence on other properties such as compression strength and fatigue behavior, these tests should be conducted in further research [27].
A subset of damaged probes were forwarded in ongoing weathering and environmental tests according to DIN EN 60068-2-38. Fractures with open flax fibers might be prone to further damage by water, due to their hydrophilic behavior [28].
The damping behavior of hybrid carbon and flax laminates will also be analyzed in detail within the project InteReSt. Our main goal is to build a horizontal tail plane and a cockpit door for an ultralight helicopter, with a high bio-based content and sufficient performance in terms of aerospace needs.

ACKNOWLEDGEMENTS

The LLB Workshop of TUM supported the practical implementation of tests and analysis.
This work was financed within the LUFO-V2 program of BMWi (Luftfahrtförderprogramm des Bundesministeriums für Forschung und Wirtschaft) in Germany.

Bundesministerium für Wirtschaft und Technologie

LITERATURE

[1] R. R. Franck, „Comparative physical, chemical and morphological characteristics of certain fibers,“ *Bast and other plant fibers,* pp. 4-23, 2005.

[2] B. Madsen and H. Lilholt, "Guidelines for mechanical design with biocomposites: properties, weight and cost," *JEC Composites Mag.,* no. No. 37, pp. 37 - 39, 2007.

[3] R. Rinberg, R. Svidler, M. Klärner, L. Kroll, K. Strohrmann, M. Hajek and H.-J. Endres, "Anwendungspotenzial von naturbasierten hybriden Leichtbaustrukturen in der Luftfahrt," in *Deutscher Luft- und Raumfahrtkongress 2016*, Braunschweig, 2016.

[4] Lineo, „TECHNICAL DATA SHEET - FLAXPLY,“ 2015.

[5] K.-R. Ramakrishnan, S. Cron, N. Le Moigne, P. Slangen and A. Bergeret, "Experimental Characterisation of the Impact Resistance of Flax Fiber Reinforced Composite Laminates," in *17th European Conference on Composite Materials*, Munich, 2016.

[6] Y. Lebaupin, M. Chauvin, T. T. Hoang and F. Touchard, "Effect of Stacking Sequence on Low Velocity Impact and Post-Impact Behavior of Flax/Polyamide 11 Composites," in *17th European Conference on Composite Materials*, Munich, 2016.

[7] U. Kling, D. Empl, O. Boegler and A. T. Isikveren, "Future Aircraft Wing Structures using Renewable Materials," in *Deutscher Luft- und Raumfahrtkongress 2015*, Rostock, 2015.

[8] F. Bensadoun, D. Depuydt, J. Baets, J. Baets and A. W. Van Vuure, "Low velocity impact properties of flax composites," *Composite Structures,* no. May-2017.

[9] L. Yan, N. Chouw and K. Jayaraman, "Flax fibre and its composites - A review," *Composites Part B: Engineering,* 2014.

[10] "BHD - more facts about our linens," Bandhni Homeware Design, 2017. [Online]. Available: http://bandhinihomeweardesign.blogspot.com/2012/06/more-facts-about-our-linens.html. [Accessed 28 08 2017].

[11] Composites Evolution Ltd, „Technical Datasheet Biotex Flax 100 g/m² 2x2 Twill,“ 2015.

[12] C. Soutis, „Fibre reinforced composites in aircraft construction,“ *Progress in Aerospace Sciences,* Bd. 41, Nr. 2, pp. 143-151, 2005.

[13] O. Boegler, A. Roth, L. Lorenz and A. Sizmann, "Assessment Framework for Sustainable Lightweight Materials in Aviation," in *Deutscher Luft- und Raumfahrtkongress 2013*, Stuttgart, 2013.

[14] A. Morasch, J. Prievitzer and H. Baier, "Zur ganzheitlichen Bewertung von Werkstoffen am beispiel von naturfaserverstärkten und glasfaserverstärkten Kunststoffen," in *Deutscher Luft- und Raumfahrtkongress 2011*, Bremen, 2011.

[15] M. F. Ashby, Materials and the Environment, Oxford: Butterworth-Heinemann, 2013.

[16] F. Sarasini, J. Tirillò, S. D'Altilia, T. Valente, C. Santulli, F. Touchard, L. Chocinski-Arnault, D. Mellier, L. Lampani and P. Gaudenzi, "Damage tolerance of carbon/flax hybrid composites subjected to low velocity impact," *Composites Part B: Engineering,* vol. 91, pp. 144-153, 2016.

[17] V. Fiore, A. Valenza and G. Di Bella, "Mechanical behavior of carbon/flax hybrid composites," *Journal of CompositeMaterials 46,* p. 2089–2096, 2012.

[18] R. Petrucci, C. Santulli, D. Puglia, E. Nisini, F. Sarasini, J. Tirillò, L. Torre, G. Minak and J. Kenny, "Impact and post-impact damage characterisation of hybrid composite laminates based on basalt fibers in combination with flax, hemp and glass fibers manufactured by vacuum infusion," *Composites Part B: Engineering 69,* p. 507–515, 2015.

[19] C. Kowtsch, C. Herzberg and R. Kleicke, Gewebte Halbzeuge und Webtechniken, vol. Textile Werkstoffe für den Leichtbau, C. C. (eds), Ed., Berlin, Heidelberg: Springer, 2011.

[20] LINEO , „LINEO - FLAX FABRICS Technical Fabrics made of Flax Fibers,“ 2010.

[21] ECC Fabrics for Composites, „Technisches Datenblatt Carbon Leinwand Style 450-5,“ 2006.

[22] G. W. Ehrenstein, Polymer-Werkstoffe, Carl Hanser, 1987.

[23] Entropy Resins Inc., „Technical Data Sheet SUPER SAP INR System,“ 2015.

[24] C. Bonten, Kunststofftechnik - Einführung und Grundlagen, Hanser Fachbuchverlag, 2016.

[25] J. Blaut, Bewertung der Widerstandsfähigkeit von hybriden Kohle-Flachs Faserverbundlaminaten

gegen Schlagbenaspruchung, Garching: Technische Universität München, 2017.

[26] H. N. Dhakal, Z. Y. Zhang, R. Guthrie, J. Mucmullen and N. Bennett, "Development of flax/carbon fibre hybrid composites for enhanced properties," *Carbohydrate Polymers 96,* pp. 1-8, 2013.

[27] T. Scalici, V. Fiore, L. Calabrese, A. Valenza and E. Proverbio, "Effect of external basalt layers on durability behaviour of flax reinforced composites," *Composites Part B: Engineering 84,* pp. 258-265, 2016.

[28] M. Bergès, R. Leger, V. Person, V. Placet, E. Ramasso, J. Rousseau, X. Gabrion, S. Corn, S. Fontaine and P. Ienny, "Effect of Moisture Uptake on Flax Fiber-Reinforced Composite Laminates: Influence on dynamic and quasi-static Properties," in *17th European Conference on Composite Materials*, Munich, 2016.